Physica C 481 (2012) 161–167

Contents lists available at SciVerse ScienceDirect

Physica C

journal homepage: www.elsevier.com/locate/physc

Quantum critical point for stripe order: An organizing principle of cuprate superconductivity

Nicolas Doiron-Leyraud, Louis Taillefer *

Département de Physique & RQMP, Université de Sherbrooke, Sherbrooke, Canada
Canadian Institute for Advanced Research, Toronto, Canada

ARTICLE INFO

Article history:
Received 24 February 2012
Received in revised form 11 April 2012
Accepted 19 April 2012
Available online 2 July 2012

Keywords:
Cuprate superconductors
Quantum critical point
Stripe order
Nematic order
Iron-based superconductors
Organic superconductors

ABSTRACT

A spin density-wave quantum critical point (QCP) is the central organizing principle of organic, iron-pnictide, heavy-fermion and electron-doped cuprate superconductors. It accounts for the superconducting T_c dome, the non-Fermi-liquid resistivity, and the Fermi-surface reconstruction. Outside the magnetically ordered phase above the QCP, scattering and pairing decrease in parallel as the system moves away from the QCP. Here we argue that a similar scenario, based on a stripe-order QCP, is a central organizing principle of hole-doped cuprate superconductors. Key properties of $La_{1.8-x}Eu_{0.2}Sr_xCuO_4$, $La_{1.6-x}Nd_{0.4}Sr_xCuO_4$ and $YBa_2Cu_3O_y$ are naturally unified, including stripe order itself, its QCP, Fermi-surface reconstruction, the linear-T resistivity, and the nematic character of the pseudogap phase.

1. Introduction

Quantum oscillations [1–6] and Hall effect [7,8] experiments on underdoped $YBa_2Cu_3O_y$ (YBCO) have revealed a small electron Fermi surface, indicative of Fermi surface reconstruction (FSR) by density-wave order [9–11]. The nature of the density-wave order, and its relation to the pseudogap and high-T_c superconductivity, are now key issues for our understanding of cuprates [12]. We have recently examined this question by looking at the response caused by the FSR in the thermoelectric properties of a number of cuprates, establishing parallels and analogies between seemingly different materials. In this article, we first discuss materials where the presence of static stripe order is convincingly established by a large body of data. These are the family of doped LSCO materials, in particular $La_{1.8-x}Eu_{0.2}Sr_xCuO_4$ (Eu-LSCO) and $La_{1.6-x}Nd_{0.4}Sr_xCuO_4$ (Nd-LSCO), which exhibit static charge-stripe order. We then turn to YBCO and show that the thermoelectric response as a function of temperature and doping is essentially identical to that of Eu-LSCO, evidence that the same mechanism of FSR, namely stripe order, is at play in both materials. Finally, we examine the full ordering process upon cooling, starting with its onset at the pseudogap temperature $T^\star$. This is where, in YBCO, the Nernst effect shows the onset of a large in-plane anisotropy, revealing the nematic character of the pseudogap phase.

* Corresponding author at: Département de Physique & RQMP, Université de Sherbrooke, Sherbrooke, Canada.
E-mail address: Louis.Taillefer@USherbrooke.ca (L. Taillefer).

0921-4534/$ - see front matter © 2012 Elsevier B.V. All rights reserved.
http://dx.doi.org/10.1016/j.physc.2012.04.040

2. Stripe order and FSR in Eu-LSCO

In Fig. 1, we show the temperature-doping phase diagram of Eu-LSCO. In this material, static charge stripe order has been observed by X-rays [13] and NQR [14] at a doping-dependent temperature T_{CO} that peaks at $p = 1/8$, but remains sizable up to at least $p = 0.20$. We emphasize that T_{CO} is well separated from other transitions, such as the structural transition that occurs near 130 K, or the superconducting T_c which never exceeds 20 K. In Fig. 2, we reproduce the X-ray intensity on Eu-LSCO at $p = 0.11$ and 0.125 as a function of temperature, which shows the onset of charge order at T_{CO}. We also display our measurements of the Seebeck coefficient S on Eu-LSCO [15,16] at the very same doping values, expressed as S over the temperature T, much like the linear-T component of specific heat. We see that S/T is small and positive at high temperature, and then drops to negative values. At low temperature, S/T becomes large and negative, indicating that it is dominated by a small electron-like Fermi surface [17]. Taking the maximum in S/T as a loose criterion for the temperature at which FSR occurs, the close correspondence between this temperature and T_{CO} is evidence that the FSR is caused by stripe order. Furthermore, a negative S/T at low temperature is only observed when stripe order is present, both being absent below $p = 0.08$, as we recently reported [16].

3. FSR and stripe order in YBCO

As shown in Fig. 2, S/T in YBCO exhibits the very same drop to negative values at low temperatures [15,16]. The magnitude of

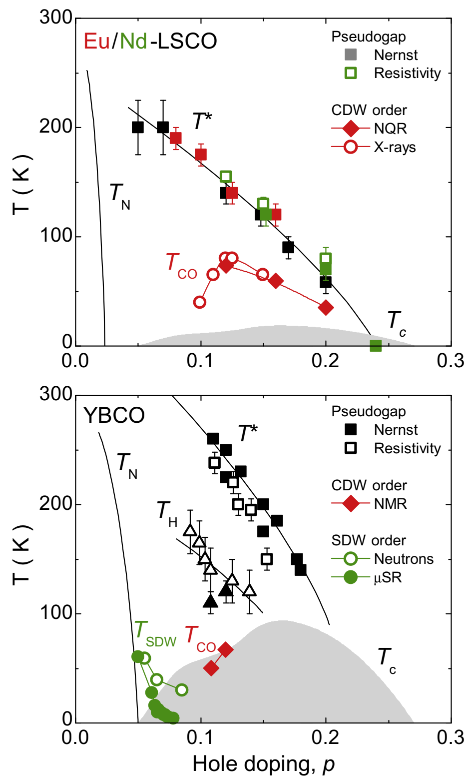

Fig. 1. Top: temperature-doping phase diagram of Nd-LSCO and Eu-LSCO. T_{CO} denotes the onset of charge density-wave order in Eu-LSCO as measured by X-rays (red circles [13]) and NQR (red diamonds [14]). The pseudogap temperature $T^{\star}$ is defined in two ways: (1) the temperature T_{ρ} (open squares) at which the electrical resistivity deviates from its high-temperature linear behaviour and (2) the temperature T_{ν} (full squares) at which the Nernst coefficient expressed as ν/T deviates from its high temperature, weakly linear, regime. T_{ρ} was extracted from resistivity data on Nd-LSCO [18,19]. T_{ν} was extracted from Nernst data on LSCO (black squares [20]), Eu-LSCO (red squares [21]), and Nd-LSCO (green squares, [21]), as reported in [22,23]. Bottom: Temperature-doping phase diagram of YBCO. T_{CO} (red diamonds) is from NMR data [24]. T_{ρ} (open squares) is from an analysis [25] of data in Ref. [26]. T_{ν} (full squares) is from Nernst data [25]. T_H is defined in the main text and is extracted in Ref. [8] from our own (full triangles) and previously published data (open triangles [27]). T_{SDW} is the onset temperature for spin density-wave order as measured by neutron scattering [28] and μSR [29]. In both panels, T_N is a schematic of the Néel temperature and T_c is the superconducting transition temperature described by the grey dome, from data in Ref. [30] for YBCO. (For interpretation of the references to colour in this figure legend, the reader is referred to the web version of this article.)

the negative residual value of S/T at $T \to 0$ is in good agreement with the magnitude expected from the small Fermi surface pocket detected by quantum oscillations [1,4], given that $S/T \propto m^{\star}/F$ [17], where F and $m^{\star}$ are the frequency and cyclotron mass of the oscillations [15,16], respectively. The dependence of S/T on both temperature and doping in Eu-LSCO and YBCO shows a detailed and striking similarity, which lead us to conclude that the FSR in YBCO is also driven by stripe order [15,16]. Recent nuclear magnetic resonance (NMR) experiments on YBCO confirmed this finding [24], revealing charge stripe order at a temperature T_{CO} which closely matches that at which the drop in S/T occurs (see Fig. 2). In Fig. 1, we reproduce the onset temperature T_{CO} measured by NMR on the phase diagram of YBCO.

Note that stripe order in Eu-LSCO exists in the absence of a magnetic field, whereas for YBCO at the dopings mentioned here ($p = 0.11$ and 0.12) static stripe order only appears when a sufficiently large magnetic field is applied. We attribute this difference to phase competition. In Eu-LSCO, owing perhaps to the more favourable crystal structure, stripe order is naturally stronger and suppresses superconductivity to a lower T_c. In YBCO, stripe order is weaker and superconductivity stronger, with a much larger T_c, therefore requiring a large magnetic field to suppress the latter and tip the balance in favour of stripe order which is otherwise suppressed.

4. Quantum critical point in Nd-LSCO

In Eu-LSCO, stripe order extends over a large portion of the temperature-doping phase diagram [13,14], as seen from the doping dependence of the onset temperature T_{CO} in Fig. 1. The very same phase diagram is observed for the closely related material Nd-LSCO [14,32]. In Nd-LSCO, we have tracked the transport properties up to the doping where stripe order vanishes, at the quantum critical point $p^{\star} = 0.24$ [33]. At this doping, we observed a strictly linear temperature dependence of the electrical resistivity (both in the plane and along the c-axis) [18], as well as a logarithmic divergence of the thermopower, $S/T \propto \log(1/T)$ [34], two archetypal signatures of a QCP [35].

This type of QCP has four principal consequences: (1) Fermi-surface reconstruction; (2) anomalous (non-Fermi-liquid) scattering; (3) unconventional pairing; and (4) phase competition. All four consequences are clearly observed in organic [36,37], pnictide [38], heavy-fermion [39–41] and electron-doped cuprate [42,43] superconductors, where the order in all cases is spin-density-wave (SDW) order. (In pnictides, the SDW order is stripe-like, i.e. unidirectional.) The dome-like region of superconductivity in the phase diagram of these four families of materials – the rise and fall of T_c – is due to pairing above, and competition below, the QCP, respectively. The linear-T resistivity at the QCP, and transport anomalies below it, are due to scattering by spin fluctuations and Fermi-surface reconstruction by SDW order, respectively. Moreover, the strength of the anomalous scattering is directly correlated with the pairing strength, in that the slope of the linear-T resistivity scales with the superconducting T_c, both decreasing in parallel as one moves away from the QCP [22]. This was observed in the organic Bechgaard salt $(TMTSF)_2PF_6$ [37], the iron-pnictide $Ba(Fe_{1-x}Co_x)_2As_2$ (Co-Ba122) [37], and the electron-doped cuprate $La_{2-x}Ce_xCuO_4$ (LCCO) [44]. The same correlation between linear-T resistivity and T_c was recently reported in the heavy fermion URu_2Si_2 [45], although in this case the nature of the QCP remains to be clarified.

The QCP at which SDW order sets in is the central organizing principle with which to understand the overall phenomenology of these superconductors. We now propose that a QCP at which stripe order sets in is a central organizing principle of hole-doped cuprates. With its QCP at $p^{\star} = 0.24$, this principle readily applies to the case of Nd-LSCO (and Eu-LSCO). Fermi-surface reconstruction is observed in several transport properties as the doping is reduced below $p^{\star}$ [18,21,34]. In Fig. 3, the normal-state electrical resistivity of Nd-LSCO at $p = 0.20$ is seen to exhibit a pronounced upturn below 40 K [18], the temperature at which NQR detects the onset of stripe order [14]. By contrast, no anomaly is seen at $p = 0.24$. What is seen instead is a perfectly linear-T resistivity as $T \to 0$, when superconductivity is suppressed by a large magnetic field [18]. This is the signature of the anomalous scattering that occurs at the QCP. The same linear-T resistivity is observed at the SDW QCP of the electron-doped $Pr_{2-x}Ce_xCuO_4$ (PCCO) [46] and LCCO [44], the organic metal $(TMTSF)_2PF_6$ [37], and the pnictides Co-Ba122 [47] and $BaFe_2(As_{1-x}P_x)_2$ (P-Ba122) [48].

In Fig. 4, we display the evolution of the electrical resistivity across three regimes typical of a quantum critical point, for a hole-doped cuprate, a Bechgaard salt, and an iron pnictide: a FSR below, linear-T at, and Fermi-liquid behavior well above, the QCP. The similarity between materials coming from different families is striking and supports the universal character of a QCP scenario.

Two questions arise. First, is this organizing principle of a stripe QCP universal amongst hole-doped cuprates? While further work is required to answer that question, two universal features would